AIAA SciTech Forum
9 - 13 January 2017, Grapevine, Texas
AIAA Guidance, Navigation, and Control Conference

A combined Averaging-Shooting Approach for the Trim Analysis of Hovering Insects/Flapping-Wing Micro-Air-Vehicles

Ahmed M. Hassan* and Haithem E. Taha†
University of California, Irvine, CA 92697

Because of the wing oscillatory motion with respect to the body, the flight dynamics of biological flyers as well as their man-made mimetic vehicles, flapping-wing micro-air-vehicles (FWMAVs), are typically represented by multi-body, nonlinear time-periodic (NLTP) system models whose balance and stability analyses are quite challenging. In this work, we consider a NLTP system model for a two-degree-of-freedom FWMAV that is confined to move along vertical rails. We combine tools from chronological calculus, geometric control, and averaging to provide a mathematically rigorous analysis for the balance of FWMAVs at hover; that is, relaxing the single-body and direct averaging assumptions that are commonly adopted in analyzing balance and stability of FWMAVs and insects. We also use optimized shooting to numerically capture the resulting periodic orbit and verify the obtained results. Finally, we provide a combined averaging-shooting approach for the balance and stability analysis of NLTP systems that (i) unlike typical shooting methods, does not require an initial guess; (ii) provides more accurate results than the analytical averaging approaches, hence relaxing the need for intractable high-order averaged dynamics; and (iii) allows a deeper scrutiny of the system dynamics, in contrast to numerical shooting methods.

I. Introduction

Flapping flight is indeed a rich dynamical system whose stability analysis and control synthesis invoke frontiers of the system dynamics and control theory. Flapping-wing micro-air-vehicles (FWMAV) are typically represented by multi-body, nonlinear, and non-autonomous dynamical system models. Moreover, these models are multi-scale dynamical systems as the body flight dynamics and wing flapping dynamics evolve on different time scales; for the slowest flapping insect (hawkmoth), the flapping frequency is almost 30 times the body flight dynamics natural frequency [1].

Two main assumptions have been typically adopted in literature (e.g., [1–11]) for control design and stability analysis of FWMAVs. The first assumption is neglecting the wing inertial effects and considering the wing as a mere lift generator, hence, reducing the dynamics to that of a single-body problem which is significantly easier in analysis. The second assumption is applying direct averaging to analyze balance and stability. Thanks to the relatively large separation between the system's two time scales, the averaging assumption is used to convert the nonlinear time-periodic (NLTP) dynamics into a nonlinear time-invariant (NLTI) one. As such, a periodic orbit representing an equilibrium configuration of the NLTP system reduces to a fixed point of the averaged dynamics. This process allows analytically tractable analysis. For a detailed literature study, the reader is referred to the review article [12] and the references therein.

As the field becomes more mature, these assumptions become refuted and should be relaxed for a proper analysis of flapping flight dynamics. While the first assumption can be justified by the fact that the wing's weight is small compared to the body (typically less than 5% [13]), Taha et al. [14] showed that the wing flapping dynamics may interact with the body flight dynamics resulting in a negative lifting mechanism. Also, Taha et al. [15] showed that the high-frequency periodic forcing due to the wing oscillatory motion may induce a vibrational stabilization mechanism on the body flight dynamics that is similar to that of the

*PhD Student, Mechanical and Aerospace Engineering. Student Member AIAA.
†Assistant Professor, Henry Samueli Career Development Chair, Mechanical and Aerospace Engineering. Member AIAA.

Stephenson-Kapitza pendulum [16–18]. That is, an unstable equilibrium may gain asymptotic stability due to the application of a sufficiently high-amplitude, high-frequency, periodic forcing [19–21]. Therefore, in contrast to the the common conclusion that FWMAVs and insects are unstable at hover [1–3, 5, 9–11], Taha et al. [15] showed the possibility of natural vibrational stabilization; such stabilizing mechanisms cannot be captured using direct averaging. This discussion motivates higher-order averaging analysis along with a multi-body formulation of the FWMAV dynamics.

In fact, the balance (trim) and stability analyses of FWMAVs are quite challenging. Whereas it is intuitive to think that vertical balance (trim) is achieved when the cycle-averaged lift due to flapping is equal to the weight, this concept has been refuted by Taha et al. [15]. It has been shown that the time-periodic aerodynamic loads interact with the system dynamics resulting in a change in the equilibrium state of the system. This phenomenon is referred to as direct/parametric interaction by Nayfeh and Mook [22]. In addition, it should be noted that while direct averaging may give non-trivial results, though inaccurate, for the single-body problem (i.e., when ignoring the wing inertia), it completely fails when the wing inertia is considered; it neglects the entire effects of flapping. Indeed, the multi-body, multi-scale, NLTP nature of the system necessitates a mathematically rigorous analysis for trim and stability, which is the main contribution of this effort.

In this work, we consider the NLTP dynamics of a two degree-of-freedom (DOF) FWMAV; a FWMAV that is restrained to move along vertical rails. The objective is to relax the common two assumptions, discussed above, and provide a mathematically rigorous analysis that results in the flapping requirements for hovering balance. To achieve such an objective, we combine tools from chronological calculus [23], geometric control [24], and averaging [25, 26]. We apply the nonlinear variation of constants (VOC) to decouple the system's two time-scales. Then, we apply first- and higher-order averaging on the resulting decoupled system. We also use an optimized shooting technique [27] to numerically capture the resulting periodic orbit and verify the obtained results. Finally we provide a combined averaging-shooting approach to analyze balance and stability of NLTP systems in general. This approach has the advantage of (i) being self-contained in the sense that, unlike typical shooting methods, it does not require an initial guess; (ii) providing a better accuracy than the analytical averaging approach without the need to perform an infeasibly high-order averaging; and (iii) allowing deeper scrutiny of the system dynamics than numerical shooting techniques.

II. Modeling

The dynamics of FWMAVs is essentially a multi-body problem. Figure 1 presents a schematic diagram for a FWMAV showing several axis-systems needed for the study; inertial frame subscripted by I, body frame subscripted by b, stroke plane frame subscripted by s, and wing frame subscripted by w. In this work, the body is constrained to move along vertical rails, as shown in the experimental setup in Fig. 2. Therefore, only two degrees of freedom are considered; the body vertical motion with a velocity w and the wing back and forth flapping angle φ; the wing pitching dynamics is ignored as typically done in FWMAVs when considering a constant pitching angle throughout each half stroke.

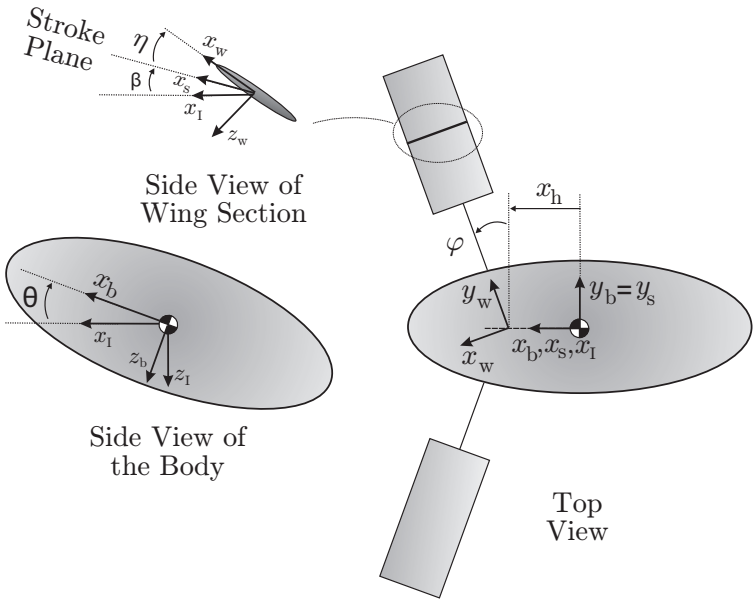

Figure 1: Schematic diagram for a FWMAV.

Using quasi-steady aerodynamic model that captures the dominant effects leading edge vortex and rotational lift contributions, Taha et al. [14] derived the longitudinal equations of motion for the body-wing multi-body dynamics using the principle of virtual power. Based on this model, we derive the

following two-DOF dynamics

$$\begin{aligned} \dot{w}(t) &= g - k_{d_1}\,|\dot{\varphi}(t)|\,w(t) - k_L\;\dot{\varphi}^2(t) \\ \ddot{\varphi}(t) &= -k_{d_2}\,|\dot{\varphi}(t)|\,\dot{\varphi}(t) - k_{d_3}\;w(t)\;\dot{\varphi}(t) + \tfrac{1}{I_F}\tau_\varphi(t), \end{aligned} \tag{1}$$

where g is the gravitational acceleration, I_F is the flapping moment of inertia, and τ_φ is the flapping control input torque. The coefficients $k_{d_1},\ k_L,\ k_{d_2}$, and k_{d_3} are defined as

$$\begin{aligned} k_{d_1} &= \frac{\rho\ C_{L_\alpha}\ I_{11}\ \cos^2\alpha_m}{2m_v} \\ k_L &= \frac{\rho\ C_{L_\alpha}\ I_{21}\ \sin\alpha_m\cos\alpha_m}{2m_v} \\ k_{d_2} &= \frac{\rho\ C_{L_\alpha}\ I_{31}\ \sin^2\alpha_m}{I_F} \\ k_{d_3} &= \frac{\rho\ C_{L_\alpha}\ I_{21}\ \sin\alpha_m\cos\alpha_m}{I_F}, \end{aligned}$$

where ρ is the air density, C_{L_α} is the wing lift curve slope, α_m is the mean angle of attack maintained throughout the entire stroke, m_v is the total mass of the vehicle, and I_{mn} are constants that depend on the chord distribution $c(r)$ of the wing: $I_{mn} = 2\int_0^R r^m c^n(r)\,dr$, where R is the wing radius. The system (1) can be written in a state-space form as

$$\frac{d}{dt}\begin{bmatrix} z(t) \\ \varphi(t) \\ w(t) \\ \dot{\varphi}(t) \end{bmatrix} = \begin{bmatrix} w(t) \\ \dot{\varphi}(t) \\ g - k_{d_1}\,|\dot{\varphi}(t)|\,w(t) - k_L\dot{\varphi}(t)^2 \\ -k_{d_2}\,|\dot{\varphi}(t)|\,\dot{\varphi}(t) - k_{d_3}w(t)\dot{\varphi}(t) \end{bmatrix} + \begin{bmatrix} 0 \\ 0 \\ 0 \\ \frac{1}{I_F} \end{bmatrix}\tau_\varphi(t), \tag{2}$$

which can be written abstractly as a typical nonlinear control-affine system

$$\dot{\boldsymbol{x}}(t) = \boldsymbol{Z}(\boldsymbol{x}(t)) + \boldsymbol{Y}(\boldsymbol{x}(t))\ \tau_\varphi(t), \tag{3}$$

where $\boldsymbol{x}(t) = [z(t) \quad \varphi(t) \quad w(t) \quad \dot{\varphi}(t)]^T$ is the state vector.

The system (1), equivalently (2), is a NLTP system because the vehicle's weight is balanced by periodic forcing (e.g., $\tau_\varphi(t) = U\cos\omega t$). The problem of determining the required amplitude U for balance (i.e., to achieve a specific periodic orbit corresponding to a desired equilibrium, e.g., hovering) is not trivial. For example, Taha et al. [15] refuted the intuitive notion that hovering is achieved by balancing the averaged flapping lift to the weight. Because the inherent stability of the system (2) due to various damping actions, any deviation from equilibrium will be attributed to unbalance. As such, because of its simplicity and implementation feasibility, the system (2) represents a paradigm for periodic orbit analysis of NLTP systems.

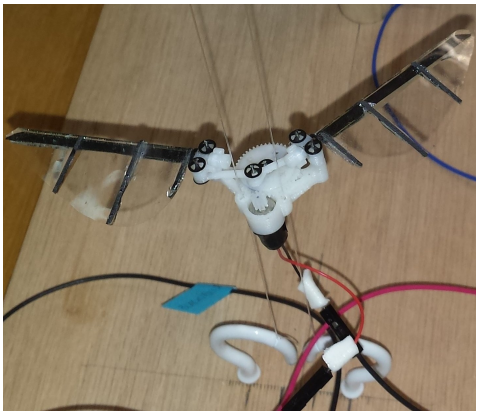

Figure 2: Experimental setup of a two DOF FWMAV.

III. Averaging Techniques

A. Averaging Theorem

Theorem 1. Consider the NLTP system

$$\dot{\boldsymbol{x}}(t) = \epsilon\boldsymbol{X}(\boldsymbol{x}(t), t). \tag{4}$$

Assuming that $\boldsymbol{X}$ is a T-periodic vector field in t, the averaged dynamical system corresponding to (4) is written as

$$\dot{\overline{\boldsymbol{x}}}(t) = \epsilon\overline{\boldsymbol{X}}(\overline{\boldsymbol{x}}(t)), \tag{5}$$

where $\overline{\boldsymbol{X}}(\overline{\boldsymbol{x}}(t)) = \frac{1}{T}\int_0^T \boldsymbol{X}(\boldsymbol{x}(t), \tau)\,d\tau$. According to the averaging theorem [28], [29]:

- If $\boldsymbol{x}(0) - \overline{\boldsymbol{x}}(0) = O(\epsilon)$, then there exist $b > 0$ and $\epsilon^* > 0$ such that $\boldsymbol{x}(t) - \overline{\boldsymbol{x}}(t) = O(\epsilon)\ \forall t \in [0, b/\epsilon]$ and $\forall \epsilon \in [0,\epsilon^*]$.
- If $\boldsymbol{x}^*$ is an exponentially stable equilibrium point of (5) and if $\|\boldsymbol{x}(0) - \boldsymbol{x}^*\| < \rho$ for some $\rho > 0$, then $\boldsymbol{x}(t) - \overline{\boldsymbol{x}}(t) = O(\epsilon)\ \forall t > 0$ and $\forall \epsilon \in [0,\epsilon^*]$. Moreover, The system (4) has a unique, exponentially stable, T-periodic solution $\boldsymbol{x}_T(t)$ with the property $\|\boldsymbol{x}_T(t) - \boldsymbol{x}^*\| \leq k\epsilon$ for some k.

Thus, the averaging approach allows converting a non-autonomous system into an autonomous system. As such, if the equilibrium state of the NLTP system is represented by a periodic orbit $\boldsymbol{x}^*(t)$, it reduces to a fixed point of the averaged dynamics. The problem of ensuring a specific periodic orbit corresponding to a desired equilibrium configuration is significantly simplified using the averaging approach, hence allowing for analytical results. Suppose the system is characterized by a vector of parameters $\boldsymbol{P}$ (e.g., U in our FWMAV example) and denote this parametric dependence as follows: $\boldsymbol{X}(\boldsymbol{x}(t), t; \boldsymbol{P})$. Without loss of generality, assume that it is required to ensure a periodic orbit $\boldsymbol{x}^*(t)$ with zero-mean (e.g., hovering equilibrium). Hence, the balance problem is stated as follows: Determine the system parameters $\boldsymbol{P}$ and the periodic orbit $\boldsymbol{x}^*(t)$ such that

$$\dot{\boldsymbol{x}^*}(t) = \boldsymbol{X}(\boldsymbol{x}^*(t), t; \boldsymbol{P}),$$

with $\overline{\boldsymbol{x}^*} = \boldsymbol{0}$. Obviously, it is not a trivial problem and often cannot be solved analytically. In contrast, the balance problem using the averaging approach is stated as follows: Determine the system parameters $\boldsymbol{P}$ that are necessary to ensure $\overline{\boldsymbol{X}}(\boldsymbol{0}; \boldsymbol{P}) = \boldsymbol{0}$. This is achieved by solving a set of algebraic equations.

One caveat we should mention before leaving this point is that the averaging theorem requires the vector field $\boldsymbol{X}(\boldsymbol{x}(t), t)$ to be smooth in all its arguments. Unfortunately, the dynamics vector field, $\boldsymbol{Z}$, in system (2) or equivalently (3), is not smooth in the state $\dot{\varphi}$ because of the absolute value function, $|\dot{\varphi}|$. We tackle this issue by introducing a smooth approximation for the absolute value function. For more details about this point, the reader is referred to an earlier work by Taha et al. [14].

B. Generalized Averaging Theory

A main issue with the averaging approach is that it is valid for small enough ϵ (i.e., for high enough frequency). Moreover, this frequency limit (determined by ϵ^*) is not known (only its existence is guaranteed). The generalized averaging theory (GAT) presents a remedy for this issue by providing an arbitrarily higher-order approximation to the flow along a time-periodic vector field. Agrachev and Gamkrelidze laid the foundation for the GAT in their seminal work [30]. Later, Sarychev [31] and Vela [32] used the concepts introduced by Agrachev and Gamkrelidze to develop a generalization for the classical averaging theorem. Only the final results of the GAT are stated here, and the reader is referred to Section 4 in [15] for a detailed presentation of the GAT. Sarychev [31] introduced the notion of complete averaging to denote the following averaged dynamics of system (4)

$$\dot{\bar{\boldsymbol{x}}}(t) = \epsilon \bar{\boldsymbol{X}}(t) = \epsilon \boldsymbol{\Lambda}_1(\bar{\boldsymbol{x}}(t)) + \epsilon^2 \boldsymbol{\Lambda}_2(\bar{\boldsymbol{x}}(t)) + \epsilon^3 \boldsymbol{\Lambda}_3(\bar{\boldsymbol{x}}(t)) + ..., \tag{6}$$

where

$$\begin{aligned}
\boldsymbol{\Lambda}_1(\bar{\boldsymbol{x}}(t)) &= \tfrac{1}{T}\int_0^T \boldsymbol{X}(\boldsymbol{x}(t), \tau) d\tau \\
\boldsymbol{\Lambda}_2(\bar{\boldsymbol{x}}(t)) &= \tfrac{1}{2T}\int_0^T \left[\int_0^t \boldsymbol{X}(\boldsymbol{x}(t), \sigma) d\sigma,\ \boldsymbol{X}(\boldsymbol{x}(t), t)\right] dt \\
\boldsymbol{\Lambda}_3(\bar{\boldsymbol{x}}(t)) &= \tfrac{T}{2}\left[\boldsymbol{\Lambda}_1(\bar{\boldsymbol{x}}(t)),\ \boldsymbol{\Lambda}_2(\bar{\boldsymbol{x}}(t))\right] + \tfrac{1}{3T}\int_0^T \left[\int_0^t \boldsymbol{X}(\boldsymbol{x}(t), \sigma) d\sigma, \left[\int_0^t \boldsymbol{X}(\boldsymbol{x}(t), \sigma) d\sigma,\ \boldsymbol{X}(\boldsymbol{x}(t), t)\right]\right] dt,
\end{aligned} \tag{7}$$

where the Lie bracket between two vector fields is defined as $[\boldsymbol{V}_1(\boldsymbol{x}), \boldsymbol{V}_2(\boldsymbol{x})] = \frac{\partial \boldsymbol{V}_2}{\partial \boldsymbol{x}}\boldsymbol{V}_1 - \frac{\partial \boldsymbol{V}_1}{\partial \boldsymbol{x}}\boldsymbol{V}_2$. Sarychev and Vela showed that if the series (6) converges, its limit will be the logarithm of the Monodromy map (i.e., the nonlinear vector-valued function that maps an initial condition to the solution after the period T). That is, if the complete averaged dynamics (6) has an exponentially stable fixed point, then the NLTP system (4) will have an exponentially stable periodic orbit, irrespective of the value of ϵ.

Based on the above discussion, it is implied that if ϵ is small enough to truncate the series after the first term, $\boldsymbol{\Lambda}_1$, the first-order averaging theorem is recovered. If not, then one should go for higher-order

averaging until the desired accuracy is met. However, only convergence of the series (6) representing the complete averaged dynamics is guaranteed under some conditions [30]. Therefore, since the series (6) is typically not asymptotic, practical computation may be an issue as one may need to perform infeasibly high-order averaging to truncate the convergent series with a good accuracy, as stressed by Nayfeh [33].

C. Nonlinear Variation of Constants Formula (VOC)

The nonlinear variation of constants formula is a useful tool for decoupling vector fields of different magnitudes and/or time-scales. In particular, it is instrumental for our analysis when the concerned nonlinear system is subjected to high-amplitude periodic forcing. In such cases, the system is not even directly amenable to the averaging theorem. Consider a nonlinear system subjected to a high-frequency, high-amplitude, periodic forcing in the form

$$\dot{\boldsymbol{x}}(t) = \boldsymbol{f}(\boldsymbol{x}(t)) + \frac{1}{\epsilon}\boldsymbol{g}(\boldsymbol{x}(t), \frac{t}{\epsilon}), \qquad \boldsymbol{x}(0) = \boldsymbol{x}_0, \tag{8}$$

where $0 < \epsilon \ll 1$. The time-varying vector field $(1/\epsilon)\boldsymbol{g}(\boldsymbol{x}(t), t/\epsilon)$ is assumed to be periodic in its second argument with period T. The system (8) is not even amenable to direct averaging, i.e., is not in the form of (4), because $\boldsymbol{f}$ and $\boldsymbol{g}$ are not of the same order. The VOC formula allows separation of the system (8) into two companion systems as follows [30], [24]

$$\begin{array}{rcll} \dot{\boldsymbol{z}}(t) & = & \boldsymbol{F}(\boldsymbol{z}(t), t), & \boldsymbol{z}(0) = \boldsymbol{x}_0 \\ \dot{\boldsymbol{x}}(t) & = & \boldsymbol{g}(\boldsymbol{x}(t), t), & \boldsymbol{x}(0) = \boldsymbol{z}(t), \end{array} \tag{9}$$

where $\boldsymbol{F}(\boldsymbol{x}(t), t)$ is the *pullback* of the vector field $\boldsymbol{f}$ along the flow $\phi_t^{\boldsymbol{g}}$ of the time-varying vector field $\boldsymbol{g}$. Using the chronological calculus formulation of Agrachev and Gamkrelidze [30], Bullo [34] showed that, for a time-invariant $\boldsymbol{f}$ and time-varying $\boldsymbol{g}$, the pullback vector field $\boldsymbol{F}(\boldsymbol{x}(t), t)$ can be written as

$$\boldsymbol{F}(\boldsymbol{x}(t), t) \quad = \quad \boldsymbol{f}(\boldsymbol{x}(t)) + \sum_{k=1}^{\infty} \int_0^t \dots \int_0^{s_{k-1}} \left(ad_{\boldsymbol{g}(\boldsymbol{x}(t),\, s_k)} \dots ad_{\boldsymbol{g}(\boldsymbol{x}(t),\, s_1)} \boldsymbol{f}(\boldsymbol{x}) \right) ds_k \dots ds_1, \tag{10}$$

where $ad_{\boldsymbol{g}}\boldsymbol{f} = [\boldsymbol{g}, \boldsymbol{f}]$. Now, if the vector field $\boldsymbol{g}$ is T-periodic in t with zero mean, the averaging of system (9) yields

$$\bar{\boldsymbol{x}}(t) = \bar{\boldsymbol{z}}(t), \quad \dot{\bar{\boldsymbol{z}}} = \bar{\boldsymbol{F}}(\bar{\boldsymbol{z}}). \tag{11}$$

Hence, in this case, one can recover the averaged dynamics of the original system (8) just by applying the averaging on the pullback vector field $\boldsymbol{F}(\boldsymbol{x}(t), t)$.

D. First Order Averaging after VOC

Theorem 2. Consider a NLTP system subject to a high-frequency, high amplitude, periodic forcing (8). Assuming that $\boldsymbol{g}$ is a T-periodic in t, zero-mean vector field and both $\boldsymbol{f}$, $\boldsymbol{g}$ are continuously differentiable, the averaged dynamical system corresponding to (8) is written as

$$\dot{\overline{\boldsymbol{x}}}(t) = \epsilon \overline{\boldsymbol{F}}(\overline{\boldsymbol{x}}(t)), \tag{12}$$

where $\overline{\boldsymbol{F}}(\overline{\boldsymbol{x}}(t)) = \frac{1}{T}\int_0^T \boldsymbol{F}(\boldsymbol{x}(t), \tau)\, d\tau$, and $\boldsymbol{F}$ is the pullback of $\boldsymbol{f}$ along the flow $\phi_t^{\boldsymbol{g}}$ of the time-varying vector field $\boldsymbol{g}$ as explained in Eq. (10). Moreover [24]:

- If $\overline{\boldsymbol{x}}(0) = \boldsymbol{x}(0)$, then there exist $b > 0$ and $\epsilon^* > 0$ such that $\boldsymbol{x}(t) - \overline{\boldsymbol{x}}(t) = O(\epsilon)$ $\forall t \in [0, b/\epsilon]$ and $\forall \epsilon \in [0, \epsilon^*]$.
- If $\boldsymbol{x}^*$ is an exponentially stable equilibrium point of (12) and if $\|\boldsymbol{x}(0) - \boldsymbol{x}^*\| < \rho$ for some $\rho > 0$, then $\boldsymbol{x}(t) - \overline{\boldsymbol{x}}(t) = O(\epsilon)$ $\forall t > 0$ and $\forall \epsilon \in [0, \epsilon^*]$. Moreover, there exists an $\epsilon_1 > 0$ such that $\forall \epsilon \in [0, \epsilon_1]$, the system (8) has a unique, ϵT-periodic, locally asymptotically stable trajectory that takes values in an open ball of radius $O(1)$ centered at $\boldsymbol{x}^*$.

The main difference between Theorem 1 (direct averaging) and Theorem 2 (VOC and averaging) is that the periodic orbit is $O(\epsilon)$ from the corresponding fixed point of the averaged dynamics in Theorem 1, while such a distance is $O(1)$ in Theorem 2. This is particularly useful in analyzing flapping flight including wing

dynamics where the flapping angle φ becomes a state variable. In this case, the small distance between the periodic changes in $\varphi(t)$ and its averaged value does not match reality; i.e., flapping flight is not typically performed with a small, $O(\epsilon)$, amplitude of flapping motion. Therefore, the application of the VOC formula is essential in analyzing flapping flight multi-body dynamics. It should be noted that Theorem 1 is not an option in this case as direct averaging would yield trivial results when applied to the system (3); i.e., it would neglect the entire effects of the flapping input vector field $\boldsymbol{Y}$.

IV. Analysis of the NLTP dynamics of a Two-DOF FWMAV

In this section, we apply the averaging techniques introduced in the last section to the two DOF FWMAV NLTP system (2) to obtain a NLTI version of it. Then, the hovering balance problem will be analyzed using the obtained averaged dynamics to determine the flapping requirements for hover.

A. Assuming a Prescribed Wing Motion

Ignoring the wing flapping dynamics (i.e., the φ-dynamics) results in the following single DOF system

$$\dot{w}(t) = g - k_{d_1} \, |\dot{\varphi}| \, (t) \; w(t) - k_L \; \dot{\varphi}(t)^2, \tag{13}$$

where the flapping angle φ is assumed to follow a cosine wave form with an amplitude Φ: $\varphi(t) = -\Phi \cos \omega t$. By applying first order averaging on the system (13) and solving for the required Φ to achieve hovering, i.e., that makes $\bar{w} = 0$ a fixed point for the averaged dynamics of the system (13), we obtain

$$\Phi_{trim} = \sqrt{\frac{2g}{k_L \omega^2}}. \tag{14}$$

which has been derived before by Doman et al. [7] and others.

Figure 3 shows a time simulation for the one DOF NLTP dynamics (13) with Φ_{trim} determined from (14) using the morphological parameters of the Hawkmoth insect, which are given in Appendix A. It is noted from Fig. 3 that the system (13) indeed goes into the hovering periodic orbit ($\bar{w} = 0$). Therefore, the first order averaging in this case is sufficient to estimate the flapping requirements.

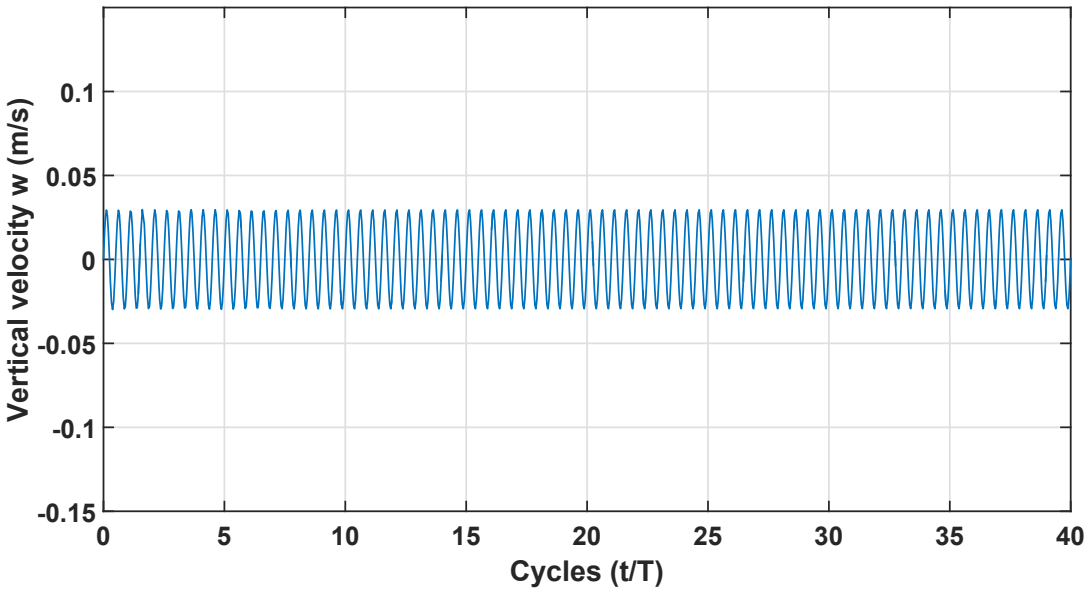

Figure 3: NLTP system response for the Hawkmoth dynamics (13) using Φ_{trim} obtained from (14) and an initial condition, $w(0) = 0$.

B. Effect of Wing Flapping Dynamics

The input to the combined body-flight-wing-flapping-dynamics (2) is the flapping torque τ_φ, which is written as

$$\tau_\varphi(t) = U\cos\omega t. \tag{15}$$

Clearly, the direct application of the averaging theorem (Theorem 1) to the system (2), with τ_φ given by (15), yields trivial results (i.e., no effect of flapping on the dynamics). Hence, we apply the VOC formula before averaging to obtain the pullback vector field which accounts for the effect of the forcing vector field on the dynamics (drift) vector filed. That is, the averaged dynamics will be determined from (11).

1. *VOC Formula with First Order Averaging*

Thanks to the mechanical structure of the system (2) and because the non-conservative forces (aerodynamic loads) are quadratic in the generalized velocities (w and $\dot\varphi$), the integral series of the pullback vector field (10) terminates after two terms. Hence, the pullback vector field can be written as

$$\boldsymbol{F}(\boldsymbol{x}(t),t) \;=\; \boldsymbol{Z}(\boldsymbol{x}(t)) + [\boldsymbol{Y},\ \boldsymbol{Z}]\int_0^t \tau_\varphi(s_1)\,ds_1 + [\boldsymbol{Y},\ [\boldsymbol{Y},\ \boldsymbol{Z}]]\int_0^t\int_0^{s_1} \tau_\varphi(s_2)\ \tau_\varphi(s_1)\,ds_2\,ds_1. \tag{16}$$

Then, we apply the averaging formulas as defined in (6) and (7) to obtain the first term in the averaging series

$$\boldsymbol{\Lambda_1}(\bar{\boldsymbol{x}}(t)) = \begin{bmatrix} w(t) \\ \dot\varphi(t) \\ g - k_L\dot\varphi(t)^2 - k_{d_1}w(t)\,|\dot\varphi(t)| + \\ +\frac{U^2}{4I_F^2\omega^2}\left(-2k_L - k_{d_1}w(t)\ \mathrm{sign}'(\dot\varphi(t))\right) \\ -k_{d_3}w(t)\dot\varphi(t) - k_{d_2}\,|\dot\varphi(t)|\,\dot\varphi(t) + \\ +\frac{U^2}{4I_F^2\omega^2}\left(-2k_{d_2}\ \mathrm{sign}(\dot\varphi(t)) - k_{d_2}\dot\varphi(t)\ \mathrm{sign}'(\dot\varphi(t))\right) \end{bmatrix}. \tag{17}$$

The first order averaged system (17) can be written in terms of the *symmetric product* of the control vector field $\boldsymbol{Y}(\boldsymbol{x})$ as [34]

$$\dot{\bar{\boldsymbol{x}}}(t) = \boldsymbol{Z}(\bar{\boldsymbol{x}}(t)) + \frac{U^2}{4\,\omega^2}\,[\boldsymbol{Y},\ [\boldsymbol{Y},\ \boldsymbol{Z}]]\,(\bar{\boldsymbol{x}}(t)). \tag{18}$$

It should be noted that because the assumed cosine waveform for τ_φ satisfies $\int_0^T\int_0^t \tau_\varphi(\sigma)d\sigma dt = 0$, application of the VOC and first-order averaging preserves the mechanical structure of the system as noted from the resulting averaged pullback vector field in (17).

To achieve balance at hover, we solve $\boldsymbol{\Lambda}_1(\boldsymbol{0}) = \boldsymbol{0}$. The third equation implies

$$U_{trim} = \sqrt{\frac{2\ gI_F^2\omega^2}{k_L}}, \tag{19}$$

while the other three equations are automatically satisfied at the origin. If the torque amplitude U is written in terms of the flapping amplitude Φ as $U = I_F\omega^2\Phi$, then Eq. (19) yields the exact same result for Φ_{trim} as Eq. (14). That is, first-order averaging on the single DOF system (13), ignoring the wing dynamics, is equivalent to first-order averaging after applying the VOC on the two DOF system (2). However, while the direct averaging approach was successful in ensuring hovering for the single DOF case, its equivalent requirements (19) in the case of multi-body dynamics is not successful in determining the right flapping torque amplitude for hover. Figure 4 shows the response of the NLTP system (2) to the oscillating $\tau_\varphi(t)$ shown in Eq. (15) with an amplitude determined from Eq. (19) using the morphological parameters of the Hawkmoth insect, which are given in Appendix A. The insect/FWMAV dynamics goes into a stable periodic orbit that is corresponding to a vertical descent at an average speed of 0.25 m/s. That is, the control input amplitude obtained from Eq. (19) is not sufficient to maintain the vehicle in the hovering periodic orbit. Hence, the VOC formula along with first order averaging cannot capture some of the interactions between the two vector fields $\boldsymbol{Y}$ and $\boldsymbol{Z}$; i.e., aerodynamic-dynamic interactions. Therefore, higher order averaging is invoked in such a case to capture these interactions.

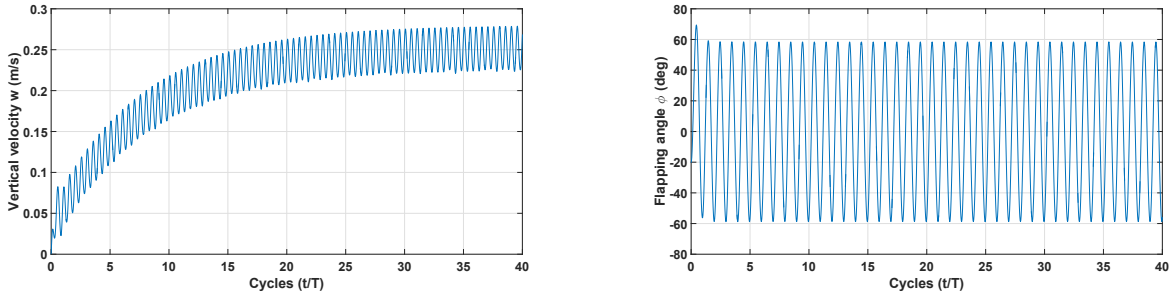

(a) w (b) φ

Figure 4: NLTP system response for the Hawkmoth dynamics (2) using U_{trim} obtained from (19) and an initial condition, $\boldsymbol{x}_0 = [0, \quad -20.3°, \quad 0, \quad 0]^T$.

It is interesting to mention that the correct balance requirement can be obtained with the above described procedure but at higher frequencies; that is, as we mentioned in Theorem 2, there is a frequency limit (signified by $1/\epsilon^*$) beyond which the obtained periodic orbit for the NLTP is guaranteed to be centered at the fixed point of the averaged system. To investigate this point more thoroughly, we double the flapping frequency and decrease the mean angle of attack α_m accordingly (almost one fourth) to maintain a similar flapping angle amplitude Φ. In this case, the aerodynamic lift due to flapping is exactly the same. This modification of the flapping parameters while maintaining the aerodynamic lift results in a pure dynamic effect. We use the same formula for flapping torque amplitude, Eq. (19), obtained through applying first order averaging after VOC. The resulting NLTP system response is shown in Fig. 5. It is noted from Fig. 5 that the average vertical velocity is almost zero (i.e., hovering balance is ensured) and the periodic orbit is centered at the fixed point equilibrium (hovering), despite $\varphi(t)$ oscillates with a relatively large amplitude, thanks to Theorem 2.

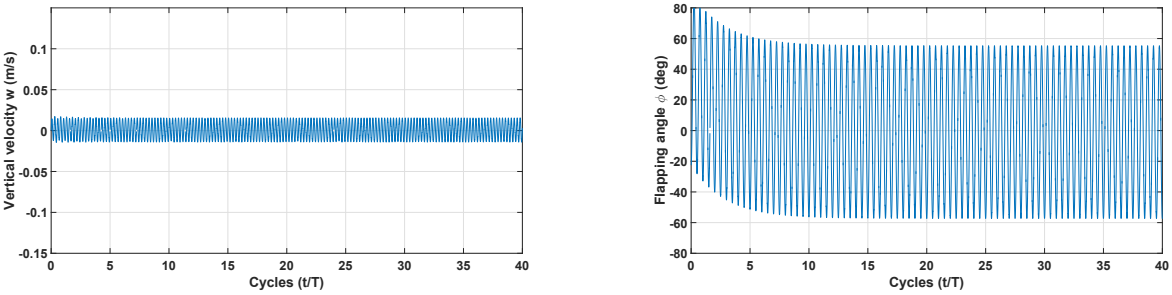

(a) w (b) φ

Figure 5: NLTP system response for the Hawkmoth dynamics (2) at higher flapping frequency (two times the recorded one) and lower α_m (one-fourth the recorded one) using U_{trim} obtained from (19) and an initial condition, $\boldsymbol{x}_0 = [0, \quad -22.5°, \quad 0, \quad 0]^T$.

2. VOC Formula with Second Order Averaging

If the frequency limit, typically dictated by averaging theorems (e.g., Theorem 2), is infeasibly high (e.g., the Hawkmoth flapping frequency is below that limit), then the trim result (19) obtained through first order averaging after VOC formula would not be sufficient to ensure the desired equilibrium periodic orbit, as discussed in the previous subsection. Hence, higher order averaging along with VOC formula is required in this case. The second term in the averaging series (6) can be obtained from the pullback vector field (16)

using the relation given in (7)

$$\boldsymbol{\Lambda}_2(\bar{\boldsymbol{x}}) = \begin{bmatrix} -\frac{T^2U}{\omega^2 I_F}\left(2k_L\dot{\varphi}(t) - k_{d_1}w(t)\ \mathrm{sign}(\dot{\varphi}(t))\right) \\ -\frac{T^2U}{\omega^2 I_F}\left(k_{d_3}w(t) + k_{d_2}\left|\dot{\varphi}(t)\right| + k_{d_2}\dot{\varphi}(t)\ \mathrm{sign}(\dot{\varphi}(t))\right) \\ \frac{T^2U}{16\omega^4 I_F^3}\Big(16I_F^2\omega^2 k_{d_3}k_{d_1}w(t)^2\mathrm{sign}(\dot{\varphi}(t)) + 8k_{d_1}k_LU^2\dot{\varphi}(t)\ \mathrm{sign}'(\dot{\varphi}(t)) - 8k_{d_2}k_LU^2\dot{\varphi}(t)\ \mathrm{sign}'(\dot{\varphi}(t)) + \\ -16I_F^2\omega^2 k_{d_1}k_{d_3}w(t)^2\dot{\varphi}(t)\ \mathrm{sign}'(\dot{\varphi}(t)) - 4k_{d_1}k_{d_2}U^2w(t)\dot{\varphi}(t)\ \mathrm{sign}'(\dot{\varphi}(t))^2 + 16gI_F^2\omega^2 k_{d_1}\mathrm{sign}(\dot{\varphi}(t)) + \\ -8k_{d_1}k_LU^2\mathrm{sign}(\dot{\varphi}(t)) - 16k_{d_2}k_LU^2\mathrm{sign}(\dot{\varphi}(t)) + 16I_F^2\omega^2 k_{d_1}k_L\dot{\varphi}(t)\left|\dot{\varphi}(t)\right| + \\ +32I_F^2\omega^2 k_{d_2}k_L\dot{\varphi}(t)\left|\dot{\varphi}(t)\right| + 32I_F^2\omega^2 k_{d_1}k_{d_2}w(t)\dot{\varphi}(t) - 8k_{d_1}k_{d_2}U^2w(t)\ \mathrm{sign}(\dot{\varphi}(t))\ \mathrm{sign}'(\dot{\varphi}(t)) + \\ -16I_F^2\omega^2 k_{d_1}k_{d_2}w(t)\dot{\varphi}(t)\left|\dot{\varphi}(t)\right|\ \mathrm{sign}'(\dot{\varphi}(t))\Big) \\ \frac{T^2U}{16\omega^4 I_F^3}\Big(16gI_F^2\omega^2 k_{d_3} - 16k_{d_2}^2U^2 - 8k_{d_3}k_LU^2 + \\ +16I_F^2\omega^2 k_{d_3}^2w(t)^2 + 16I_F^2\omega^2 k_{d_3}k_L\dot{\varphi}(t)^2 + 32I_F^2\omega^2 k_{d_2}^2\dot{\varphi}(t)^2 - 4k_{d_3}k_{d_1}U^2w(t)\ \mathrm{sign}'(\dot{\varphi}(t)) + \\ +12k_{d_3}k_{d_2}U^2w(t)\ \mathrm{sign}'(\dot{\varphi}(t)) - 16I_F^2\omega^2 k_{d_3}k_{d_2}w(t)\dot{\varphi}(t)^2\ \mathrm{sign}'(\dot{\varphi}(t)) + 8k_{d_2}^2U^2\left|\dot{\varphi}(t)\right|\ \mathrm{sign}'(\dot{\varphi}(t)) + \\ -4k_{d_2}^2U^2\dot{\varphi}(t)^2\ \mathrm{sign}'(\dot{\varphi}(t))^2 + 32I_F^2\omega^2 k_{d_3}k_{d_2}w(t)\left|\dot{\varphi}(t)\right| - 16I_F^2\omega^2 k_{d_2}^2\dot{\varphi}(t)^2\left|\dot{\varphi}(t)\right|\ \mathrm{sign}'(\dot{\varphi}(t))\Big) \end{bmatrix}. \tag{20}$$

Apparently, as noted from the first two elements in (20), the mechanical structure of the averaged system is ruined after second order averaging. However, the first two equations of the balance requirements

$$\boldsymbol{\Lambda}_1(\mathbf{0}) + \boldsymbol{\Lambda}_2(\mathbf{0}) = \mathbf{0},$$

are automatically satisfied. Moreover, the third equation yields the same balance requirement, U_{trim}, as given in Eq. (19). That is, the second order averaging does not contribute to the balance problem. This invokes third order averaging.

3. VOC Formula with Third Order Averaging

Applying third-order averaging, as shown in Eq. (7), on the pullback vector field (16), we obtain too lengthy and complicated expressions for the averaged dynamics to show here. Moreover, the mechanical structure is completely ruined. As such, a pure analytical solution becomes hard to find. Since the mechanical structure is ruined, i.e., the first two equations in the averaged system are not trivial, trim analysis at nonzero $\bar{\dot{\varphi}}$ might be required. From the multiple solutions of the nonlinear set of algebraic equations for trim, we considered only those complying with the physics of the problem. The most feasible solution when compared with the numerical value resulting from Eq. (19) can be written as

$$U_{trim_{3rd}} = 1.0463\sqrt{\frac{2\ gI_F^2\omega^2}{k_L}}. \tag{21}$$

Figure 6 shows the simulation of the NLTP dynamics (2) of the Hawkmoth using the input torque amplitude obtained form Eq. (21). The FWMAV's descent velocity is significantly decreased from 0.25 m/s to 0.02 m/s. That is, the obtained equilibrium is closer to the hovering periodic orbit where w oscillates with a zero-mean. This implies the ability of third order averaging of more accurately capturing the aerodynamic-dynamic interactions and determining the appropriate balance requirements. However, if more accurate trim results are needed, higher-order averaging would be required, which may be impractical to carry out.

V. Numerical Approach

In this section, a numerical approach to capture a periodic orbit of the two-DOF reduced order model is shown. There are two main purposes of this section; first, to validate the results obtained by the averaging

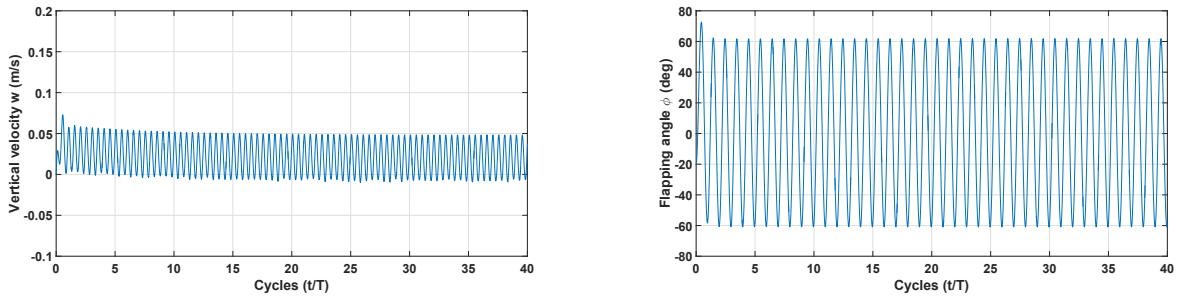

(a) w (b) φ

Figure 6: NLTP system response for the Hawkmoth dynamics (2) using U_{trim} obtained from (21) and an initial condition, $\boldsymbol{x}_0 = [0, \quad -20.3°, \quad 0, \quad 0]^T$.

approach, second, to provide a combined averaging-shooting approach for the balance and stability analysis of NLTP systems. The sought approach is intended to (i) exploit the accuracy of numerical shooting methods in comparison to the analytical averaging approaches, hence, relaxing the need for intractably high-order averaging, and (ii) allow usage of the analytical tractability of averaging to scrutinize the dynamical behavior of the system.

A. Optimized Shooting Method for Capturing a Periodic Solution

Dednam and Botha [27] provided an optimized shooting approach to capture a periodic solution of a nonlinear system. Due to its simplicity in comparison to collocation methods, we adopt such an optimized shooting approach in this work. Unlike common shooting methods where a set of ordinary differential equations are solved to minimize the residual function, the Levenberg-Marquardt optimization algorithm is adopted here. This algorithm is based on two methods: the gradient descent method and the Gauss-Newton method. According to Gavin [35], when the parameters are far from the optimal values, the Levenberg-Marquardt algorithm operates in a way similar to gradient-descent. However, it operates similar to Gauss-Newton method when approaching the optimal point.

Consider the following system of equations

$$\dot{\boldsymbol{x}}(t) = \boldsymbol{f}(\boldsymbol{x}(t), \boldsymbol{\alpha}, t), \tag{22}$$

where $\boldsymbol{x} \in \mathbb{R}^n$ and $\boldsymbol{f}$: $\mathbb{R}^n \times \mathbb{R}^k \times \mathbb{R}_{\geq 0} \to \mathbb{R}^n$, and $\boldsymbol{\alpha}$ are the system parameters. This system corresponds to a non-autonomous vector field. Thus, a solution $\boldsymbol{x}(t)$ to the system (22) is periodic if there exists a constant $T > 0$ such that

$$\boldsymbol{x}(t) = \boldsymbol{x}(t + T). \tag{23}$$

The optimized shooting method can be applied to any system that can be expressed in the form of (22), and, for convenience, a dimensionless time τ is introduced such that $t = \tau\, T$. Equation (22) is then written as

$$\frac{d\boldsymbol{x}}{d\tau} = \mathrm{T}\boldsymbol{f}(\boldsymbol{x}(\tau \mathrm{T}), \boldsymbol{\alpha}, \tau \mathrm{T}). \tag{24}$$

Thus, this new variable τ allows the simplification of the boundary conditions in Eq. (23) so that $x(\tau = 0) = x(\tau = 1)$ and Eq. (24) can be integrated over one period (i.e., letting τ run from zero to one). Now, the residual can be written as

$$\mathbf{R} = T \int_0^1 \boldsymbol{f}(\boldsymbol{x}(\tau \mathrm{T}), \boldsymbol{\alpha}, \tau \mathrm{T})\; d\tau. \tag{25}$$

According to Dednam and Botha [27], the residual depends on the number of quantities to be optimized and can be expressed as

$$\mathbf{R} = \Big(\boldsymbol{x}(1) - \boldsymbol{x}(0),\; \boldsymbol{x}(1 + \Delta\tau) - \boldsymbol{x}(\Delta\tau), \ldots,\; \boldsymbol{x}(1 + (p-1)\Delta\tau) - \boldsymbol{x}((p-1)\Delta\tau)\Big), \tag{26}$$

where $\Delta\tau$ is the integration step size and $p \in \mathbb{N}$. The natural number p in the residual equation is a requirement of the Levenberg-Marquardt algorithm and has to be chosen so that the number of components of the residual is greater than or equal to the number of quantities to be optimized. Note that the number of components in the residual function is given by pN, where N is the dimension of the system. Thus, the objective will be to find a point on the periodic orbit, $\boldsymbol{x}(0)$, that minimizes the residual.

B. Application

1. *Descent Periodic Orbit Due to First-Order Averaging with VOC*

In this subsection, the optimized shooting method is applied on the NLTP system (1) using flapping torque amplitude U_{trim} from Eq. (19) due to first-order averaging and VOC. The resulting point on the periodic solution is

$$\begin{aligned} w(0) &= 0.277\ m/s \\ \dot{\phi}(0) &= 49.48\ rad/s, \end{aligned} \tag{27}$$

which, when given as initial condition to the numerical integrator, results in the periodic orbit shown in Fig. 8. That is, a vertical descent periodic solution, with $\bar{w} \simeq 0.25\ m.s^{-1}$, is captured, which is expected based on the previous discussions and simulations shown in Fig. 4. In other words, first order averaging after VOC formula is not sufficient to determine the exact balance requirements and consequently ensure the desired periodic orbit. In addition, we present a simulation of the NLTP system (1) with zero initial condition ($w(0) = 0\ m/s$ and $\dot{\phi}(0) = 0\ rad/s$) in Fig. 7, which shows the transient phase before reaching the stable periodic orbit.

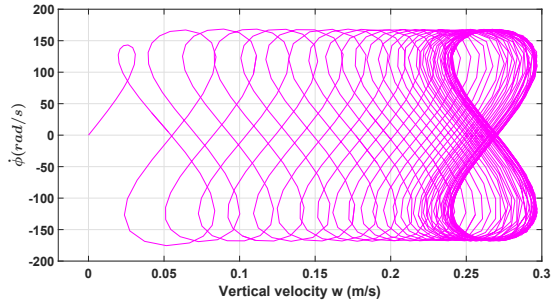

Figure 7: System trajectories using $U_{trim_{1st}}$ with zero-initial conditions.

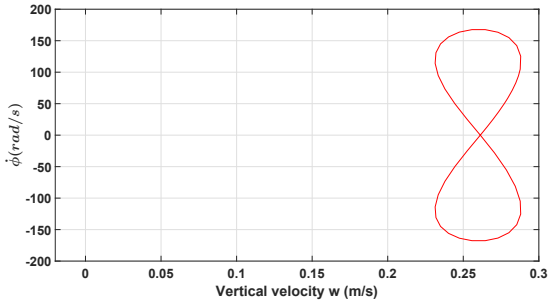

Figure 8: The corresponding periodic orbit to $U_{trim_{1st}}$.

2. *A Close-to-Hover Periodic Orbit Due to Third-Order Averaging with VOC*

In this subsection, the optimized shooting method is applied on the NLTP system (1) using flapping torque amplitude U_{trim} from Eq. (21) due to third-order averaging and VOC. The resulting point on the periodic solution is

$$\begin{aligned} w(0) &= 0.033188\ m/s \\ \dot{\phi}(0) &= 50.32\ rad/s, \end{aligned} \tag{28}$$

which, when given as initial condition to the numerical integrator, results in the periodic orbit shown in Fig. 10. That is, a vertical descent periodic solution, with $\bar{w} \simeq 0.02\ m.s^{-1}$, is captured, which is expected based on the previous discussions and simulations shown in Fig. 6. In other words, third order averaging after VOC formula is still not sufficient to determine the exact balance requirements and consequently ensure the desired periodic orbit. In addition, we present a simulation of the NLTP system (1) with zero initial condition ($w(0) = 0\ m/s$ and $\dot{\phi}(0) = 0\ rad/s$) in Fig. 9, which shows the transient phase before reaching the stable periodic orbit.

C. Solving for U_{trim} Simultaneously with the Periodic Orbit

In this subsection, we use the same numerical technique (optimized shooting) to simultaneously obtain the trim requirements to ensure a desired periodic orbit (e.g., hovering) along with capturing the periodic orbit

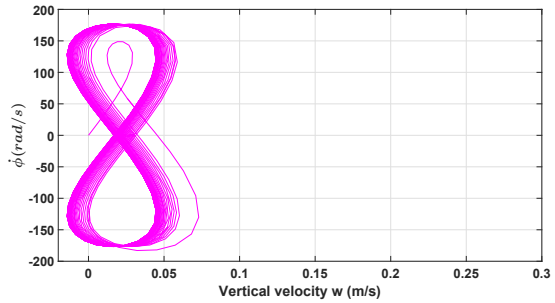

Figure 9: System trajectories using $U_{trim_{3rd}}$ and zero-initial conditions.

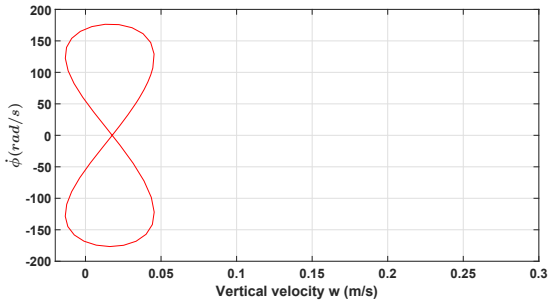

Figure 10: The corresponding periodic orbit to $U_{trim_{3rd}}$.

itself. This is achieved by considering the parameter U_{trim} as a variable rather than an input to the algorithm and adding one more equation to the optimized shooting algorithm that ensures that the found periodic orbit is indeed the hovering one. More precisely, we require

$$\bar{w} = 0 \quad \Leftrightarrow \quad z(0) = z(T) \tag{29}$$

which is equivalent to requesting a periodic solution for the state z representing the vertical displacement of the FWMAV.

Applying the optimized shooting method on the two DOF FWMAV system (1) with the additional constraint (29), and starting the algorithm with an initial guess for U_{trim} as obtained from averaging approaches ($U_{trim_{1st}}$ or $U_{trim_{3rd}}$), we obtain the following results

$$\begin{aligned} w(0) &= 0.0177\ m/s \\ \dot{\phi}(0) &= 50.3857\ rad/s, \end{aligned} \tag{30}$$

with a flapping input torque amplitude

$$U_{trim_{exact}} = 1.05169 \sqrt{\frac{2\ gI_F^2\omega^2}{k_L}}. \tag{31}$$

Figure 11 shows a time simulation of the NLTP system (1) with zero-initial conditions and $U_{trim_{exact}}$. It is noted from Fig. 11 that the system tends rapidly (after around 20 cycles) to an average vertical velocity value which is very close to *zero*, i.e., a hovering periodic orbit. Fig. 12 shows a similar simulation with an initial point on the periodic orbit as resulting from the optimized shooting method, i.e., Eq. (30).

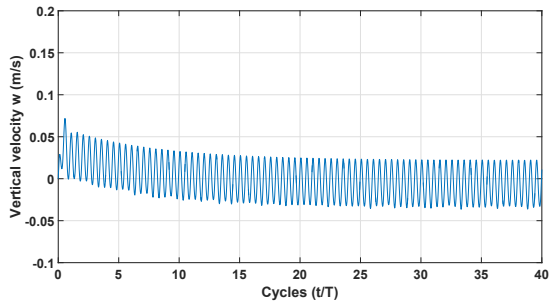

Figure 11: Vertical velocity w using $U_{trim_{exact}}$ for 40 cycles.

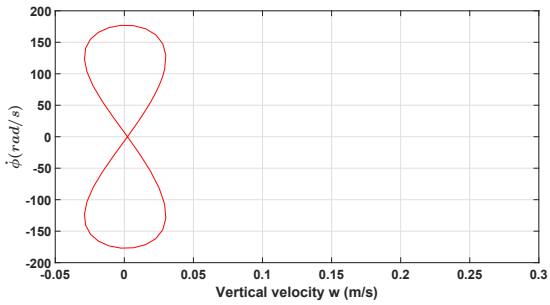

Figure 12: The corresponding periodic orbit to $U_{trim_{exact}}$.

D. Discussion

One might argue that if the optimized shooting method yields the accurate balance requirements for hovering (an accurate U_{trim}) then the analytical averaging techniques might not be necessary. To address this

argument we mention here two important points. First, the optimized shooting method explained above is not guaranteed to yield the correct results if it is started at any arbitrary initial guess. The initial guess has to be close enough to the correct result, and this is where the proposed self-contained combined averaging-shooting approach proves its effectiveness. Second, the work presented in this paper is a first part of an effort that aims at analyzing not just the balance of FWMAVs but also the stability characteristics. Although FWMAVs stability could be investigated numerically through Floquet theory after a periodic orbit is captured, but this would only yield a yes/no answer to the stability question without any insights as to why this system has been rendered stable/unstable and what are the stabilizing/destabilizing mechanisms. On the other hand, using the accurate balance requirements obtained from the proposed combined averaging-shooting approach and feeding it back to the averaging procedure to obtain a linearized averaged system at a specific equilibrium point would allow us to scrutinize the stability characteristics of the system in order to gain insights into different stabilizing/destabilizing mechanisms (e.g., positive/negative stiffness) and to reveal any potential unconventional stabilizing mechanism (e.g., vibrational stabilization). Finally, Fig. 13 summarizes the analysis procedure and results in this paper.

VI. Conclusions

In this paper, we considered a reduced order model for a two-degree-of-freedom flapping-wing micro-air-vehicle (FWMAV) that is confined to move along vertical rails. We relaxed the two common assumptions (neglecting wing inertia and performing direct-averaging) usually adopted in the balance and stability analysis of FWMAVs and insects. We noted that while direct averaging provides non-trivial results, though inaccurate, when ignoring the wing inertial effects, it completely fails if this assumption is relaxed; it neglects the entire flapping effects. To overcome this predicament, we provided a mathematically rigorous analysis for the balance and stability of FWMAVs by combining tools from chronological calculus, geometric control, and averaging. In particular, the balance problem (i.e., ensuring a specific periodic orbit corresponding to a desired equilibrium) was investigated. The nonlinear variation of constants (VOC) formula was found to be a necessary tool to analyze such a multi-body, multi-time-scale dynamical system. However, we found that applying first-order averaging after the nonlinear VOC formula is not capable of capturing

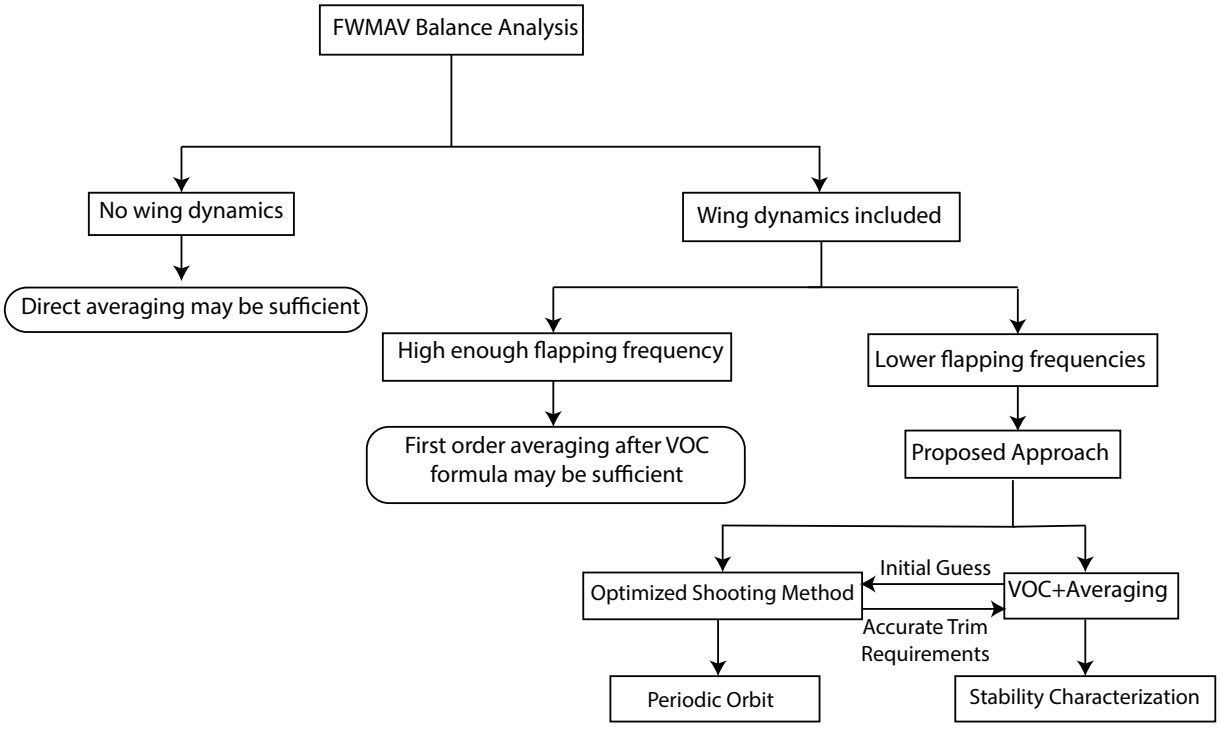

Figure 13: A schematic for the analysis procedure and results in this paper.

the aerodynamic-dynamic interactions in the considered system (flapping frequency is not high enough) as manifested by a persistent drift from the hovering periodic orbit. Applying third-order averaging after the VOC formula (as second-order averaging does not contribute to the balance problem), we achieved a periodic orbit that is considerably closer to the desired hovering periodic orbit. Additionally, we showed that if the considered system has high enough frequency, applying first-order averaging after the VOC formula would be enough to ensure the correct balance requirement.

On the other hand, an optimized shooting method was adopted to numerically capture the resulting periodic orbits. To circumvent providing an accurate initial guess as needed by shooting methods, we proposed combining the averaging approach with the shooting method; the result of first-order averaging after the VOC formula is a convenient initial guess. The shooting method was then used to determine a more accurate estimate for the hovering balance flapping requirements than those resulting from higher-order averaging. Moreover, these requirements (flapping parameters) can then be fed to the analytically determined higher-order averaged dynamics to scrutinize the dynamical behavior of the system for discovery of potential unconventional stabilizing mechanisms (vibrational stabilization), which will be considered in a future work by the authors. As such, the proposed combined averaging-shooting approach has the advantage of (i) being self-contained in the sense that, unlike typical shooting methods, it does not require an initial guess; (ii) providing more accurate results than the analytical averaging approaches, hence relaxing the need for intractable high-order averaged dynamics; and (iii) allowing a deeper scrutiny of the system dynamics, in contrast to the numerical shooting methods.

Appendix

A. Hawkmoth Morphological Parameters

The morphological parameters and the wing planform for the hawkmoth, as given in [1] and [36], are

$$R = 51.9\text{mm},\ \mathrm{S} = 947.8\text{mm}^2,\ \bar{c} = 18.3\text{mm},$$
$$\hat{r}_1 = 0.44,\ \hat{r}_2 = 0.525,\ f = 26.3\text{Hz},\ \Phi = 60.5^\circ,$$
$$\alpha_m = 30^\circ,\ m_b = 1.648\text{gm},\ \text{and}\ \mathrm{I_{yb}} = 2080\text{mg.cm}^2,$$

where R is the semi-span of the wing, S is the area of one wing, $\bar{c}$ is the mean chord, f is the flapping frequency, Φ is the flapping angle amplitude, m_b is the mass of the body, and I_{yb} is the body moment of inertia around the body y-axis. The moments of the wing chord distribution $\hat{r}_1$ and $\hat{r}_2$ are defined as

$$I_{k1} = 2\int_0^R r^k c(r)\,dr = 2SR^k\hat{r}_k^k.$$

As for the wing planform, the method of moments used by Ellington [36] is adopted here to obtain a chord distribution for the insect that matches the documented first two moments $\hat{r}_1$ and $\hat{r}_2$; that is,

$$c(r) = \frac{\bar{c}}{\beta}\left(\frac{r}{R}\right)^{\lambda-1}\left(1-\frac{r}{R}\right)^{\gamma-1},$$

where

$$\lambda = \hat{r}_1\left[\tfrac{\hat{r}_1(1-\hat{r}_1)}{\hat{r}_2^2-\hat{r}_1^2}-1\right],\ \gamma = (1-\hat{r}_1)\left[\tfrac{\hat{r}_1(1-\hat{r}_1)}{\hat{r}_2^2-\hat{r}_1^2}-1\right],$$
$$\text{and}\ \ \beta = \textstyle\int_0^1 \hat{r}^{\lambda-1}(1-\hat{r})^{\gamma-1}\,d\hat{r}.$$

The mass of one wing is taken as 5.7% of the body mass according to Wu et al. [13] and is assumed uniform with an areal mass distribution m' The inertial properties of the wing are then estimated as

$$I_x = 2\textstyle\int_0^R m' r^2 c(r)\,dr\ ,\ I_y = 2\int_0^R m'\hat{d}^2 c^3(r)\,dr$$
$$, I_z = I_x + I_y,\ \text{and}\ r_{\mathrm{cg}} = \frac{2\int_0^R m' r c(r)\,dr}{m_{\mathrm{w}}} = \frac{I_{11}}{2S},$$

where $\hat{d}$ is the chord-normalized distance from the wing hinge line to the center of gravity line. The parameters used in system (2) are then evaluated as

$$k_{d_1} = 0.0353739,\ k_L = 0.000621676,$$
$$k_{d_2} = 0.333915,\ k_{d_3} = 16.5766$$
$$\text{and}\ I_F = 1.37801 * 10^{-7}.$$

Acknowledgments

The authors would like to thank Matthieu Robart for his help with the numerical approach. Also, the authors gratefully acknowledge the support of the National Science Foundation grants CMMI-1435484 and CMMI-1709746, and program manager Dr. Jordan Berg.

References

[1] Sun, M., Wang, J., and Xiong, Y., "Dynamic Flight Stability of Hovering Insects," *Acta Mechanica Sinica*, Vol. 23, No. 3, 2007, pp. 231–246.

[2] Taylor, G. K. and Thomas, A. L. R., "Animal Flight Dynamics II. Longitudinal Stability in Flapping Flight," *Journal of Theoretical Biology*, Vol. 214, 2002.

[3] Taylor, G. K. and Thomas, A. L. R., "Dynamic Flight Stability in the Desert Locust," *Journal of Theoretical Biology*, Vol. 206, 2003, pp. 2803–2829.

[4] Khan, Z. A. and Agrawal, S. K., "Control of Longitudinal Flight Dynamics of a Flapping Wing Micro Air Vehicle Using Time Averaged Model and Differential Flatness Based Controller," IEEE American Control Conference, 2007, pp. 5284–5289.

[5] Sun, M. and Xiong, Y., "Dynamic flight stability of a hovering bumblebee." *Journal of Experimental Biology*, Vol. 208, No. 3, 2005, pp. 447–459.

[6] Xiong, Y. and Sun, M., "Dynamic Flight Stability of a Bumble Bee in Forward Flight," *Acta Mechanica Sinica*, Vol. 24, No. 3, 2008, pp. 25–36.

[7] Doman, D. B., Oppenheimer, M. W., and Sigthorsson, D. O., "Wingbeat Shape Modulation for Flapping-Wing Micro-Air-Vehicle Control During Hover," *Journal of Guidance, Control and Dynamics*, Vol. 33, No. 3, 2010, pp. 724–739.

[8] Oppenheimer, M. W., Doman, D. B., and Sigthorsson, D. O., "Dynamics and Control of a Biomimetic Vehicle Using Biased Wingbeat Forcing Functions," *Journal Guidance, Control and Dynamics*, Vol. 34, No. 1, 2011, pp. 204–217.

[9] Faruque, I. and Humbert, J. S., "Dipteran insect flight dynamics. Part 1 Longitudinal motion about hover," *Journal of theoretical biology*, Vol. 264, No. 2, 2010, pp. 538–552.

[10] Gao, N., Aono, H., and Liu, H., "A Numerical Analysis of Dynamic Flight Stability of Hawkmoth Hovering," *Journal of Biomechanical Science and Engineering*, Vol. 4, No. 1, 2009, pp. 105–116.

[11] Cheng, B. and Deng, X., "Translational and Rotational Damping of Flapping Flight and Its Dynamics and Stability at Hovering," *IEEE Transactions On Robotics*, Vol. 27, No. 5, 2011, pp. 849–864.

[12] Taha, H. E., Hajj, M. R., and Nayfeh, A. H., "Flight Dynamics and Control of Flapping-Wing MAVs: A Review," *Nonlinear Dynamics*, Vol. 70, No. 2, 2012, pp. 907–939.

[13] Wu, J. H., Zhang, Y. L., and Sun, M., "Hovering of model insects: simulation by coupling equations of motion with Navier-Stokes equations," *The Journal of Experimental Biology*, Vol. 212, No. 20, 2009, pp. 3313–3329.

[14] Taha, H. E., Woolsey, C. A., and Hajj, M. R., "Geometric Control Approach to Longitudinal Stability of Flapping Flight," *Journal of Guidance, Control, and Dynamics*, Vol. 39, No. 2, 2016, pp. 214–226.

[15] Taha, H. E., Tahmasian, S., Woolsey, C. A., Nayfeh, A. H., and Hajj, M. R., "The need for higher-order averaging in the stability analysis of hovering, flapping-wing flight," *Bioinspiration & biomimetics*, Vol. 10, No. 1, 2015, pp. 016002.

[16] Stephenson, A., "On Induced Stability," *The London, Edinburgh, and Dublin Philosophical Magazine and Journal of Science*, Vol. 15, No. 86, 1908, pp. 233–236.

[17] Kapitsa, P., "Pendulum with a vibrating suspension," *Uspekhi Fiz. Nauk*, Vol. 44, No. 1, 1951, pp. 7–20.

[18] Kapitsa, P., "Dynamical stability of a pendulum when its point of suspension vibrates," *Collected Papers by PL Kapitsa*, Vol. 2, 1965, pp. 714–725.

[19] Meerkov, S. M., "Principle of vibrational control: theory and applications," *Automatic Control, IEEE Transactions on*, Vol. 25, No. 4, 1980, pp. 755–762.

[20] Bellman, R., Bentsman, J., and Meerkov, S. M., "On vibrational stabilizability of nonlinear systems," *Journal of optimization theory and applications*, Vol. 46, No. 4, 1985, pp. 421–430.

[21] Bellman, R. E., Bentsman, J., and Meerkov, S. M., "Vibrational control of nonlinear systems: Vibrational stabilizability," *Automatic Control, IEEE Transactions on*, Vol. 31, No. 8, 1986, pp. 710–716.

[22] Nayfeh, A. H. and Mook, D. T., *Nonlinear Oscillations*, John Wiley and Sons, Inc., 1979.

[23] Agrachev, A. A. and Gamkrelidze, R. V., "The exponential representation of flows and the chronological calculus," *Mathematics of the USSR: Sbornik*, Vol. 35, No. 6, 1979, pp. 727–785.

[24] Bullo, F. and Lewis, A. D., *Geometric control of mechanical systems: modeling, analysis, and design for simple mechanical control systems*, Vol. 49, Springer Science & Business Media, 2004.

[25] Bullo, F., "Averaging and vibrational control of mechanical systems," *SIAM Journal on Control and Optimization*, Vol. 41, No. 2, 2002, pp. 542–562.

[26] Vela, P. A., *Averaging and Control of Nonlinear Systems (with Application to Biomimetic Locomotion)*, Ph.D. thesis, California Institute of Technology, Pasadena, CA, May 2003.

[27] Dednam, W. and Botha, A., "Optimized shooting method for finding periodic orbits of nonlinear dynamical systems," *Engineering with Computers*, Vol. 31, No. 4, 2015, pp. 749–762.

[28] Guckenheimer, J. and Holmes, P., *Nonlinear oscillations, dynamical systems, and bifurcations of vector fields*, Vol. 42, Springer Science & Business Media, 2013.

[29] Sanders, J. A., Verhulst, F., and Murdock, J. A., *Averaging methods in nonlinear dynamical systems*, Vol. 59, Springer, 2007.

[30] Agrachev, A. A. and Gamkrelidze, R. V., "The exponential representation of flows and the chronological calculus," *Matematicheskii Sbornik*, Vol. 149, No. 4, 1978, pp. 467–532.

[31] Sarychev, A., "Stability criteria for time-periodic systems via high-order averaging techniques," *Nonlinear control in the year 2000 volume 2*, Springer, 2001, pp. 365–377.

[32] Vela, P. A., *Averaging and control of nonlinear systems*, Ph.D. thesis, California Institute of Technology, 2003.

[33] Nayfeh, A. H., *Perturbation Methods*, John Wiley and Sons, Inc., 1973.

[34] Bullo, F., "Averaging and vibrational control of mechanical systems," *SIAM Journal on Control and Optimization*, Vol. 41, No. 2, 2002, pp. 542–562.

[35] Gavin, H., "The Levenberg-Marquardt method for nonlinear least squares curve-fitting problems," *Department of Civil and Environmental Engineering, Duke University*, 2011, pp. 1–15.

[36] Ellington, C. P., "The aerodynamics of hovering insect flight: II. Morphological parameters," *Philosophical Transactions Royal Society London Series B*, Vol. 305, 1984, pp. 17–40.